SEMARAK ILMU PUBLISHING

CFD Letters

Journal homepage:
https://semarakilmu.com.my/journals/index.php/CFD_Letters/index
ISSN: 2180-1363

Numerical Investigation of Thermal Performance Enhancement in a Newly Designed Shell and Tube Heat Exchanger using TiO_2 Nanofluids

Muiz Abdul Raqib[1], Yaser Alaiwi [1], Ahmad Jundi[1,*]

[1] Department of Mechanical Engineering, Altinbas University, Istanbul, Turkey

ARTICLE INFO

Article history:
Received 7 March 2024
Received in revised form 10 April 2024
Accepted 9 May 2024
Available online 30 September 2024

Keywords:
CFD; Nano-fluid; Investigate; Thermal performance; Analysis

ABSTRACT

This study investigates the use of titanium dioxide (TiO_2) nanofluids to enhance the thermal performance of shell and tube heat exchangers. A comparative computational fluid dynamics (CFD) analysis is conducted using water and a 0.5% TiO_2 nanofluid. The heat exchanger is modelled using computer-aided design (CAD), with dimensions closely resembling commercial units. The CFD model is validated through a grid-independence study, with a mesh of 4,112,679 elements yielding grid-independent results. The key findings show that the 0.5% TiO_2 nanofluid increases the cold fluid outlet temperature by 11.44% compared to water (36.04°C vs. 33.63°C). The average heat transfer coefficient is enhanced by 12.3% when using the nanofluid. The CFD results are consistent with experimental data, with a maximum deviation of 4.2% in the outlet temperatures. This study demonstrates the successful integration of TiO_2 nanofluids with an optimized shell and tube heat exchanger design. The novelty lies in the application of nanofluids to improve the thermal performance of industrial heat exchangers. The presented methodology, combining CAD modelling and CFD analysis, provides a foundation for further optimization and experimental validation of nanofluid-enhanced heat transfer systems.

1. Introduction

Heat exchangers have emerged as indispensable components enabling optimized thermal management and efficient energy utilization across vital industrial domains like manufacturing, power generation, food processing, pharmaceuticals, and more. They facilitate productive transmission of heat between fluids, ensuring precise temperature control critical for product quality, safety compliance and prolonged equipment lifespan. Specifically, heat exchangers contribute substantially to heightened energy efficiency by capturing waste heat for recycling instead of dissipation. This greatly reduces overall energy expenses and environmental footprint aligning with sustainability objectives. Their small, lightweight build suits space constraints in facilities. Heat exchangers prevent cross-contamination through isolated fluid channels, upholding purity standards in industries like pharmaceuticals. Quick, productive waste heat recovery using minimal additional

* *Corresponding author.*
E-mail address: ahmad.t.jundi@gmail.com (Ahmad Jundi)

https://doi.org/10.37934/cfdl.17.2.6082

inputs also attests their effectiveness. Furthermore, the versatility of heat exchangers tackling diverse thermal demands makes them vital across chemical plants, refineries, and HVAC infrastructure among myriad applications. Their affordability compared to alternatives provides a compelling value proposition when optimizing heating and cooling systems. Therefore, improving heat exchanger performance through modern research promises to unlock major efficiency gains leading to greener, cost-effective industrial operations, cementing their indispensable present and future role across sectors [1].

Heydari *et al.,* [2] performed a numerical analysis to study the effect of using different nanofluids on the performance of a baffled shell-and-tube heat exchanger. Nanofluids containing nanoparticles like Al_2O_3, CuO, and Fe_2O_3 dispersed in base fluids water and ethylene glycol were modeled at various concentrations. The results showed a reduction in heat transfer coefficient by 5-15%, heat transfer rate by 3-12%, and pressure drop by 10-25% while increasing outlet temperature by 2-5% when using nanofluids. Analysis also showed that ethylene glycol-based nanofluids provided 3-8% higher effectiveness than water-based ones. Overall, the researchers concluded that adding nanoparticles to the fluid inside the heat exchanger, despite reducing the heat transfer coefficient, pressure drop and heat transfer rate, increases the outlet temperature. Rani *et al.,* [3] reviewed studies on applying nanofluids in crossflow heat exchangers. They explained that crossflow heat exchangers work more efficiently than shell & tube, spiral and plate types owing to higher heat transfer rates. Performance can be further improved by using nanofluids containing metal oxide nanoparticles suspended in water. The paper discusses analytical, numerical, experimental, and artificial neural network studies analysing the performance of such nanofluid-based heat exchangers. Factors like nanoparticle type and concentration, tube diameter, fin spacing, etc. were evaluated to optimize the designs. The results showed a noticeable enhancement in convective heat transfer when nanofluids were used instead of conventional heat transfer fluids. Specifically, suspending metal oxide nanoparticles in water provided the best improvements in heat transfer rates. Kareemullah *et al.,* [4] performed an experimental analysis on a shell-and-tube heat exchanger utilizing zinc oxide nanofluids, aiming to analyse the potential heat transfer enhancements offered by nanofluids. They conducted a comparative assessment against water to evaluate parameters like heat transfer coefficient and overall efficiency. The mass flow rate on the tubes was adjusted while maintaining fixed shell-side rates. Outcomes exhibited effectiveness improvements with growing nanofluid mass flow. This evidence the ability of tailored nanofluids to intensify heat transfer in such heat exchangers. Attributed to factors like higher viscosities, the heightened transfer rates come coupled with pumping power penalties. Still, within suitable operating ranges, zinc oxide nanofluids proved capable of augmenting both heat recovery and effectiveness. The study thus substantiates the viability of nanofluid-based shell-and-tube exchangers following decisive real-world testing. It also underscores the need to holistically weigh heat transfer improvements against related costs for feasible adoption. Lahari *et al.,* [5] conducted a study on enhancing heat transfer in hairpin heat exchangers using TiC, MgO, and Ag/water-glycerin nanofluids. They performed analytical investigations to evaluate the performance of these nanofluids at different volume concentrations, using water and glycerin as base fluids. The study utilized CFD analysis to determine heat transfer coefficients and rates, indicating that Ag/water-glycerin nanofluid exhibited the highest heat transfer rate among the tested fluids. V.Ghazanfari *et al.,* [6] conducted a study focusing on the role of nanofluids in boosting heat exchanger performance through 3-D computational fluid dynamics (CFD). The research aimed at optimizing twisted tubes by varying pitch lengths, with validation achieved by comparing with prior experimental and numerical data. Key findings revealed that nanofluids significantly enhance heat transfer in twisted tubes, albeit with a slight increase in pressure drop, particularly when using 0.1 vol% Cu and 0.15 vol% Al_2O_3 nanoparticles. This enhancement suggests a

promising potential for nanofluid application in improving heat exchanger efficiency and offers insights for the design and optimization of heat transfer systems across various industrial applications. Hussein and Alaiwi [7] presented extensive experimentation published in X journal analyzing titanium dioxide/water nanofluids for enhancing counterflow double-pipe heat exchanger effectiveness across various nanoparticle concentrations from 0.1-0.5%. Detailed instrumentation measured resulting changes in thermophysical properties like thermal conductivity and viscosity alongside heat transfer metrics across different flow rates. Outcomes displayed over 20% thermal conductivity and 15% viscosity growth with nanofluid incorporation, translating to major heat transfer coefficient and efficiency spikes above baseline levels before declining at higher concentrations. Peak effectiveness was recorded at 0.3% concentration, with heat transfer rates of 17% over pure water. The research further correlated efficiencies to parameters including heat transfer units and Reynolds numbers. Demonstrating sizable real-world performance gains from judiciously tailored nanofluids, it makes vital contributions toward their adoption in sustainable heat exchange equipment across industries. V. Ghazanfari *et al.,* [8] explore the application of waterAl_2O_3 nanofluid as a coolant in annular fuels for a typical VVER-1000 reactor. Through thermal-hydraulic modeling, their research highlights the potential of Al_2O_3 nanofluid to significantly enhance heat transfer efficiency. This could lead to lower coolant flow rates, improving the operational safety and efficiency of nuclear reactors. Their work underscores the importance of nanofluids in advancing nuclear reactor cooling technologies, with computational fluid dynamics (CFD) analysis playing a key role in their findings.

The research gap centers on exploring the thermal performance of shell-and-tube heat exchangers enhanced with TiO_2 nanofluids, emphasizing a pioneering design methodology. Unlike preceding studies, this research innovates by engineering a design from the ground up using computational tools, ensuring that while dimensions mirror practical market ranges, they are distinct and optimized for the specific interaction with TiO_2 nanofluids. This approach not only aligns with commercial viability but also ventures beyond existing models to exploit nanofluids' thermal benefits fully, thus addressing a nuanced gap in optimizing heat exchanger efficiency and application.

This study aims to assess the efficacy of TiO_2 nanofluids in boosting heat transfer within shell and tube heat exchangers, motivated by the urgent need for more efficient heat recovery systems in industrial settings. Leveraging the exceptional properties of nanofluids, the research seeks innovative methods to enhance heat transfer and minimize energy consumption. The study will involve the development of a 3D CAD model of the heat exchanger, slightly differing in dimensions from those commercially available. This deviation allows for the exploration of a new design, potentially optimizing performance beyond current standards. By comparing the use of TiO_2 nanofluid with traditional water through this bespoke model, the study evaluates improvements in heat transfer. CFD simulations will further elucidate flow and temperature distributions, pinpointing areas for heat transfer enhancement and potential design optimization. The goal is to showcase the advantages of nanofluid-enhanced heat exchangers in terms of energy efficiency and sustainability, laying the groundwork for future developments in heat exchange technologies and their industrial applications.

Section 2 presents the methodology, including the theoretical background, CAD design of the shell and tube heat exchanger, and the numerical analysis using computational fluid dynamics (CFD). Section 3 discusses the results obtained from the CFD simulations for both case studies, comparing the performance of the heat exchanger with pure water and the TiO_2 nanofluid. Finally, Section 4 concludes the paper, summarizing the key findings and outlining future research directions.

2. Methodology

This section outlines the approach used to investigate the effectiveness of TiO_2 nanofluids in enhancing heat transfer within a shell and tube exchanger. The methodology starts by establishing the theoretical foundation, covering fundamental heat transfer equations and their application in heat exchanger analysis. The study then discusses the design of a unique shell and tube heat exchanger using SOLIDWORKS. While the overall dimensions resemble those of commercial units, the design introduces custom modifications, particularly in the tube spacing, to explore potential performance improvements when coupled with nanofluids. The properties and preparation of the TiO_2 nanofluid are also presented, with a focus on the 0.5% volume concentration used in the analysis. The nanofluid's characteristics are compared to those of pure water, which serves as the baseline fluid. The core of the methodology lies in the Computational Fluid Dynamics (CFD) simulations, conducted using SOLIDWORKS Flow Simulation. The governing equations for fluid flow and heat transfer are presented, alongside the boundary conditions and simulation setup for the two case studies: pure water and the TiO_2 nanofluid.

A grid independence test is performed before the main analysis to ensure the accuracy and reliability of the results. This test establishes the optimal mesh resolution that balances computational efficiency and solution precision. The simulation procedure includes mesh generation, specification of boundary conditions, and the assignment of material properties. The section provides a step-by-step guide to the CFD analysis, from pre-processing to post-processing. By the end of this section, readers will have a comprehensive understanding of the integrated approach used to assess the performance of TiO_2nanofluids in the custom-designed shell and tube heat exchanger. The methodology, based on theoretical principles and advanced computational tools, sets the stage for the presentation and discussion of the results.

2.1 Heat Transfer Science

Heat transfer refers to analyzing and quantifying the exchange of thermal energy across physical systems, focusing specifically on transfer rates rather than net heat quantities over time. It encompasses three primary mechanisms – conduction, convection, and radiation [9].

2.1.1 Conduction

Refers to the process where heat energy is transmitted through a material due to the presence of a temperature gradient, driven by the microscopic collisions among its particles. The principle underlying conduction is encapsulated by Fourier's law, which, when applied to one-dimensional heat flow through a solid, is formulated as [10]:

$$q'' = -k\frac{dT}{dx} \tag{1}$$

Where q'' is the heat flux, k is the thermal conductivity, and $\frac{dT}{dx}$ is the temperature gradient.

2.1.2 Convection

This covers the process of heat exchange between a stationary solid surface and a fluid in motion next to it, which is achieved through the combined effects of molecular diffusion and the fluid's large-

scale flow. The mathematical representation of this heat transfer mechanism is captured by the convection rate equation, commonly referred to as Newton's law of cooling [10]:

$$q'' = h(T_s - T_\infty) \tag{2}$$

Where h is the convection heat transfer coefficient, T_s is the surface temperature, and T_∞ is the fluid temperature.

2.1.3 Radiation

Radiation is the emission of energy from a substance in the form of electromagnetic waves or photons due to its thermal state. The Stefan-Boltzmann law quantifies the total energy radiated per unit area over the entire spectrum, given by the following equation [10] :

$$q'' = \epsilon\sigma(T^4 - T_{\text{surroundings}}^4) \tag{3}$$

Here, q'' is the radiant heat flux (W/m^2), ϵ is the surface's emissivity, σ is the Stefan-Boltzmann constant. T is the absolute temperature of the emitting surface and $T_{\text{surroundings}}$ is the absolute temperature of the surrounding environment.

2.2 Heat Exchanger Types

Heat exchangers are crucial devices used to transfer heat between fluids at different temperatures across various industries. They are classified based on the transfer mechanism, flow arrangement, construction, and phase of fluids. Common designs include shell-and-tube, plate, plate-fin, spiral plate, and direct contact exchangers. The choice depends on the application, fluid properties, fouling tendencies, and cost. Key design objectives relate to accommodating thermal stresses, enabling maintenance, minimizing inventory, and optimizing costs. Heat exchangers have enabled modern power plants, desalination, food processing, and chemical processes. Recent research focuses on enhancing heat transfer coefficients while minimizing fouling [11]. Figure 1 and Figure 2 below show two types of famous heat exchangers.

Fig. 1. Double pipe heat exchanger (a) Parallel flow (b) Counterflow [10]

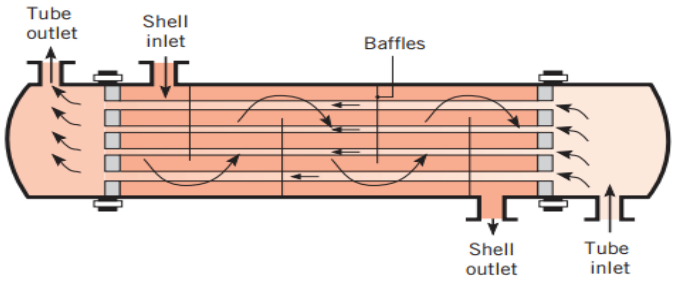

Fig. 2. Schematic for shell and tube heat exchanger [10]

2.2.1 Shell and tube heat exchanger theoretical equations

i. Heat Duty: The amount of thermal energy transferred between fluids to achieve desired temperature changes, defined by the formula [12]:

ii.

$$Q_S = M_S \cdot c_S \cdot (T_1 - T_2) \tag{4}$$

$$Q_T = M_T \cdot c_T \cdot (t_2 - t_1) \tag{5}$$

Where, $\mathrm{Q_S}$, $\mathrm{Q_T}$ are the heat transferred in the shell and tube sides (W), $\mathrm{M_S}$, $\mathrm{M_T}$ are the mass flow rates of the fluids (kg/h), $\mathrm{c_S}$,$\mathrm{c_T}$ are the specific heat capacities (Wh/kg·K), $\mathrm{T_1}$, $\mathrm{t_1}$ are the inlet temperatures (°C), and $\mathrm{T_2}$, $\mathrm{t_2}$ are the outlet temperatures (°C) of the fluids in the shell and tube sides, respectively.

iii. Overall Heat Transfer Coefficient (U) Calculation [12]:

$$Q = U \cdot A \cdot \Delta T_m \tag{6}$$

iv. log mean temperature difference [10]:

$$q = UA\Delta T_{\mathrm{lm}} \tag{7}$$

Where,

$$\Delta T_{\mathrm{lm}} = \frac{\Delta T_2 - \Delta T_1}{\ln(\Delta T_2/\Delta T_1)} = \frac{\Delta T_1 - \Delta T_2}{\ln(\Delta T_1/\Delta T_2)} \tag{8}$$

For the parallel-flow exchange [10]:

$$\begin{bmatrix} \Delta T_1 = T_{h,1} - T_{c,1} = T_{h,i} - T_{c,i} \\ \Delta T_2 = T_{h,2} - T_{c,2} = T_{h,o} - T_{c,o} \end{bmatrix} \tag{9}$$

Where $\mathrm{T_{h,i}}$ is the inlet temperature of the hot fluid, $\mathrm{T_{c,i}}$ is the temperature of the cold fluid, $\mathrm{T_{h,o}}$ is the outlet temperature of the hot fluid. $\mathrm{T_{c,o}}$ is the outlet temperature of the cold fluid. All the units are degrees Celsius (°C).

For the counter-flow exchange [10]:

$$\begin{bmatrix} \Delta T_1 = T_{h,1} - T_{c,1} = T_{h,i} - T_{c,o} \\ \Delta T_2 = T_{h,2} - T_{c,2} = T_{h,o} - T_{c,i} \end{bmatrix} \tag{10}$$

Heat exchanger effectiveness [10]:

The efficiency, denoted ε, is defined as the proportion of the actual rate of heat transfer in a heat exchanger compared to the highest achievable rate of heat transfer [10].

$$\varepsilon = \frac{q}{q_{max}} \tag{11}$$

2.3 Nanofluids

Nanofluids are heat transfer fluids containing suspended nanoparticles (< 100 nm) in base fluids like water, ethylene glycol, or oil. Developed in 1995, nanofluids exhibit superior thermal conductivity and heat transfer performance compared to base fluids alone, even at low volume fractions (< 5%). Nanoparticles are stabilized using surfactants, surface functionalization, or physical methods. Nanofluids have potential applications in transportation cooling, industrial processes, microelectronics, defence systems, nuclear systems, and solar water heating. They offer significant heat transfer enhancements and compact thermal management solutions across various fields [13].

2.3.1 Advantages of employing nanofluids

The use of nanofluids as heat transfer fluids in heat exchangers provides several important Nanofluids with nanoparticles in them that have better thermophysical properties than regular heat transfer fluids. This means that the heat transfer coefficient and rate are much better in heat exchangers when using nanofluids. This allows the heat exchangers to transfer heat more effectively and achieve a higher efficiency of operation. Additionally, the improved heat transfer performance means that lower mass flow rates of nanofluids may be required, or smaller-sized heat exchangers that achieve the same heat duty can be designed. This directly translates to reductions in pumping power requirements and material costs for construction. The nanofluids also open new possibilities for compact heat exchanger designs aimed at recovering low-grade waste heat from industrial effluents and exhaust gases and reusing it for heating applications. Overall, the economic and performance studies show that nanofluids have commercially acceptable properties compared to their cost, which makes them a good choice for engineered heat transfer fluids. e significantly enhanced thermophysical properties of nanofluids can allow better utilization of heat exchangers, lower operating costs, more compact installation footprints, and possibilities for waste heat recovery, ultimately contributing to saving energy [14].

2.3.2 Challenges and disadvantages of nanofluids

One of the main challenges in using nanofluids in heat exchangers is maintaining the long-term stability of nanoparticle dispersions, as aggregation over time can reduce their thermal performance. Additionally, the higher viscosity and density of nanofluids lead to increased pressure drop and pumping power requirements, particularly under turbulent flow conditions. Inconsistencies in the thermal performance of nanofluids have also been reported, with some studies showing no improvement or even deterioration in convective heat transfer under turbulent flow and reduced enhancement in fully developed regions. Finally, the high cost of nanofluids, due to the advanced equipment needed for production and the cost of nanoparticles themselves, remains a significant barrier to their practical application in heat exchangers [15].

2.3.3 Nano fluid concentration analysis

i. Thermal Conductivity (Maxwell model): The Maxwell model is used to estimate the effective thermal conductivity of nanofluid [16].

$$k_{nf} = k_{bf}\left(\frac{k_{np}+2k_{bf}-2\phi(k_{bf}-k_{np})}{k_{np}+2k_{bf}+\phi(k_{bf}-k_{np})}\right) \quad (12)$$

Where,k_{nf} is the thermal conductivity of the nanofluid (W/m·K), k_{bf} is the Thermal conductivity of the base fluid (W/m·K), k_{np} is the Thermal conductivity of the nanoparticles (W/m·K), and ϕ Volume fraction of nanoparticles (dimensionless).

ii. Viscosity (Einstein model) The Einstein model predicts the increase in viscosity due to the dispersed particles [17].

$$\mu_{nf} = \mu_{bf}(1 + 2.5\phi) \tag{13}$$

Where, μ_{nf} is the dynamic viscosity of the nanofluid (Pa·s), μ_{bf} is the Dynamic viscosity of the base fluid (Pa·s), ϕ is the volume fraction of nanoparticles (dimensionless), and (1+2.5ϕ) is the correction factor for the presence of nanoparticles.

iii. Specific Heat Capacity (Mixture Rule): The mixture rule is applied to calculate the nanofluid's specific heat capacity [18].

$$C_{p,nf} = \phi C_{p,np} + (1 - \phi)C_{p,bf} \tag{14}$$

Where,$C_{p,nf}$ is specific heat capacity of the nanofluid (J/kg·K), $C_{p,np}$ is specific heat capacity of the nanoparticles (J/kg·K), and $C_{p,bf}$ is specific heat capacity of the base fluid (J/kg·K).

iv. Density (Mixture Rule): The mixture rule for densities provides an estimate for the nanofluid's density [19].

$$\rho_{nf} = \phi\rho_{np} + (1 - \phi)\rho_{bf} \tag{15}$$

Where, ρ_{nf} is density of the nanofluid (kg/m³),ρ_{np} is density of the nanoparticles (kg/m³), and ρ_{bf} is density of the base fluid (kg/m³).

2.4 Computational Fluid Dynamics

The convergence of physics, mathematics, and computer science in the 1970s gave birth to computational fluid dynamics (CFD), a field focused on simulating fluid flows. The development of CFD has been closely tied to advancements in computing power, enabling the progression from modelling simple 2D flows to complex 3D simulations involving turbulence, combustion, and real gas effects. Significant milestones include solving non-linear potential equations for transonic airflow, Euler equations for inviscid flows, and Navier-Stokes equations with various turbulence models like direct numerical simulation (DNS) and large eddy simulation (LES). Improved numerical methods and grid generation techniques have allowed CFD to handle geometric complexity and enhance simulation fidelity across diverse applications in engineering and science. Despite its widespread use, CFD still faces challenges in areas such as turbulence modelling, combustion, heat transfer, and robust discretization. While advances in computing power have made complex CFD simulations possible on personal computers, further research is needed to address open questions and explore new opportunities in design optimization using CFD [20].

2.4.1 Governing equations

The foundational principles of fluid dynamics and thermodynamics are encapsulated within the governing equations that address fluid flow and heat transfer. Rooted in the fundamental conservation laws of physics—specifically, the conservation of mass, momentum, and energy—these equations characterize how a fluid behaves by detailing its macroscopic characteristics like velocity, pressure, density, and temperature, along with how these properties change across space and over time [21].

i. Continuity equation:

$$\frac{\partial \rho}{\partial t} + \nabla \cdot (\rho \mathrm{u}) = 0 \tag{16}$$

Where ρ is the fluid density (mass per unit volume), t: Time. u: velocity vector of the fluid, and $\nabla \cdot (\rho \mathrm{u})$ divergence of the mass flux, indicating how much mass is entering or leaving a point in space.

ii. Momentum Equations in space [21]:

For the x-component:

$$\rho \frac{Du}{Dt} = -\frac{\partial p}{\partial x} + \frac{\partial \tau_{xx}}{\partial x} + \frac{\partial \tau_{yx}}{\partial y} + \frac{\partial \tau_{zx}}{\partial z} + S_{Mx} \tag{17}$$

For the y-component:

$$\rho \frac{Dv}{Dt} = -\frac{\partial p}{\partial y} + \frac{\partial \tau_{xy}}{\partial x} + \frac{\partial \tau_{yy}}{\partial y} + \frac{\partial \tau_{zy}}{\partial z} + S_{My} \tag{18}$$

For the z-component:

$$\rho \frac{Dw}{Dt} = -\frac{\partial p}{\partial z} + \frac{\partial \tau_{xz}}{\partial x} + \frac{\partial \tau_{yz}}{\partial y} + \frac{\partial \tau_{zz}}{\partial z} + S_{Mz} \tag{19}$$

Where, Du/Dt , Dv/Dt, Dv/Dt are substantive derivatives of the velocity components in the x, y, and z directions, representing the acceleration of a fluid particle, S_{Mx}, S_{My}, S_{Mz} are Source terms for momentum in the x, y, and z directions, representing external forces (e.g., gravity, electromagnetic forces) per unit volume, $\tau_{xx}, \tau_{yx}, \tau_{zx}$.

iii. Energy Equation [21]

$$\rho \frac{De}{Dt} = -\nabla \cdot q + \nabla \cdot (\tau \cdot \mathrm{u}) - \nabla p \cdot \mathrm{u} + S_E \tag{20}$$

Where *e* is the specific internal energy of the fluid, q is the heat flux vector, representing the rate of heat transfer per unit area, $\tau \cdot \mathrm{u}$ is the work done by viscous stresses, indicating how viscous forces contribute to the energy change, S_E is the source term for energy, representing external heat sources or sinks per unit volume.

2.5 Shell and Tube Heat Exchanger CAD Design and Numerical Analysis

This section aims to design a heat exchanger using SOLIDWORKS, a computer-aided design (CAD) software. The design will follow the shell and tube configuration. A review of standard market dimensions will be carried out to select dimensions that are similar but not identical to existing designs. The design process will take inspiration from a reference design, which will be adapted to incorporate new features that improve its performance. To provide a clear representation of the design's details, SOLIDWORKS Composer will be used to generate visual representations, highlighting important dimensions and other relevant information. This approach will streamline the design process and ensure that the final product is a well-engineered solution.

After completing the design, a computational fluid dynamics (CFD) analysis will be performed using Flow Simulation, which is integrated within SOLIDWORKS. This analysis will provide valuable insights into the heat exchanger's performance, allowing for the evaluation of key parameters such as fluid flow patterns, temperature distributions, and pressure drop across the device. By utilizing Flow Simulation, we can identify potential areas for improvement and optimize the design to enhance its efficiency and effectiveness. The CFD study will also enable us to visualize and understand the complex fluid dynamics occurring within the heat exchanger, supporting data-driven decision-making throughout the design process. The results obtained from this analysis will be essential in validating the design and ensuring that it meets the desired performance criteria before proceeding to the manufacturing stage.

2.5.1 Shell and tube heat exchanger model design

Figure 3 below shows a complete model of the shell-and-tube heat exchanger, following its comprehensive design using SOLIDWORKS software. Figure 4 illustrates the heat exchanger after a section has been extracted, providing a clear view of its internal pipes and baffles.

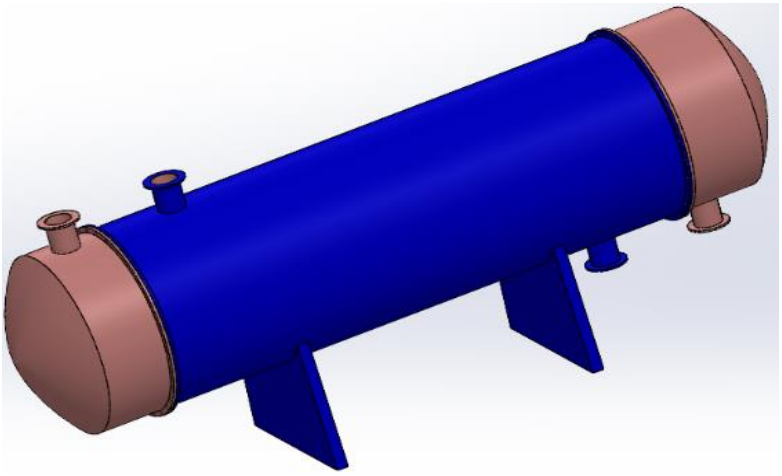

Fig. 3. Final model of the shell and tube heat exchanger

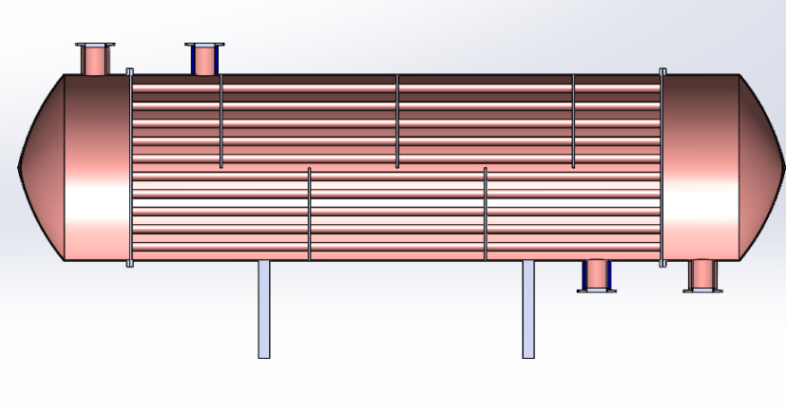

Fig. 4. 2D section of the shell and tube heat exchanger

The Figure 5, Figure 6, and Figure 7 below show the geometry dimensions of the heat exchanger by SOLIDWORKS Composer.

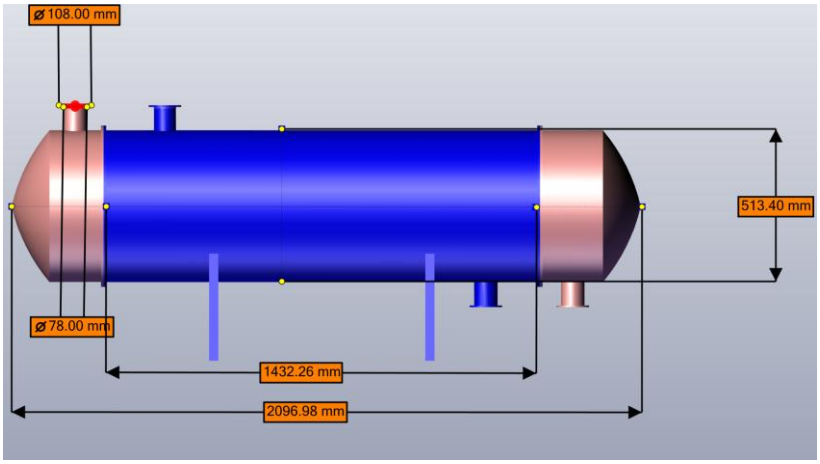

Fig. 5. Shell and tube heat exchanger dimensions for the outer shell and inlets and outlets

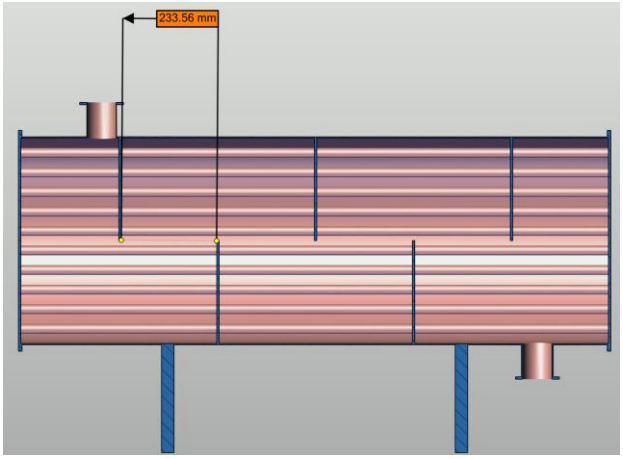

Fig. 6. Shows the number of baffles and the distance between them

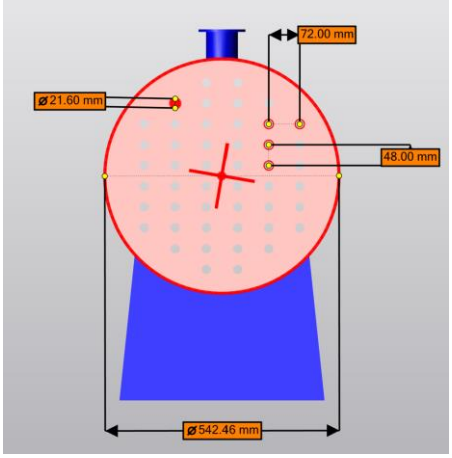

Fig. 7. Shell and tube heat exchanger dimensions for inner tubes

All dimensions and parameters related to the shell and tube heat exchanger are shown in Table 1 below.

Table 1
Main dimensions and geometry parameters of the model

Parameter	Value
Total length	2096.98 m
Shell diameter	513.40 mm
Tube length	1432.26 mm
Horizontal distance between tubes	72 mm
Vertical distance between tubes	48 mm
Number of tubes	48
Tube Diameter	21.6 mm
Inlets and outlet diameter	78 mm
Flange diameter	108 mm
Number of baffles	5
Baffle cut	50%
Distance between baffles	233.56 mm

2.5.2 Numerical analysis using flow simulation

i. Mesh analysis

Grid independence testing is crucial for designing optimal meshes in CFD simulations. It involves assessing solution accuracy on progressively refined grids to identify the mesh resolution beyond which the solution remains essentially unchanged. This process establishes a grid-independent solution that strikes a balance between accuracy and computational cost. Grid independence testing eliminates the need for subjective judgment in mesh selection by providing an objective guideline for mesh density. By quantifying discretization errors using metrics such as the grid convergence index (GCI), this testing ensures that the CFD solution closely approximates the true continuous equations and physical flows while minimizing spatial errors. Achieving a grid-independent solution is vital for obtaining reliable CFD results. The article examines an improved testing approach that determines the optimal grid resolution based on geometrical characteristics. Ultimately, formal grid

independence testing enhances confidence in CFD predictions by verifying the spatial convergence of the numerical approximation [22].

In SOLIDWORKS' Flow Simulation module, mesh generation is automated, enabling the autonomous division of cells. Users can select a refinement level ranging from 1 to 7. For this project, levels 1 to 7 will be used to determine the optimal mesh configuration, which is defined as the mesh that produces a stable output that does not change significantly with further refinement.

The Table 2 below shows the number of cells generated by the program at each refinement level from 1 to 7.

Table 2
Refinement level vs. number of cells generation

Refinement level	Number of cells
1	45816
2	71428
3	734358
4	1029859
5	2989859
6	4112679
7	9419425

In the next section, the results obtained from the grid test will be presented. This will include the representation of the cold fluid's temperature upon exit, i.e., after heating, for each 'number of cells' in every case. From this, the optimum mesh will be determined.

The Figure 8 below shows the mesh results on the heat exchanger as a whole and specifically on the tubes at the third refinement level.

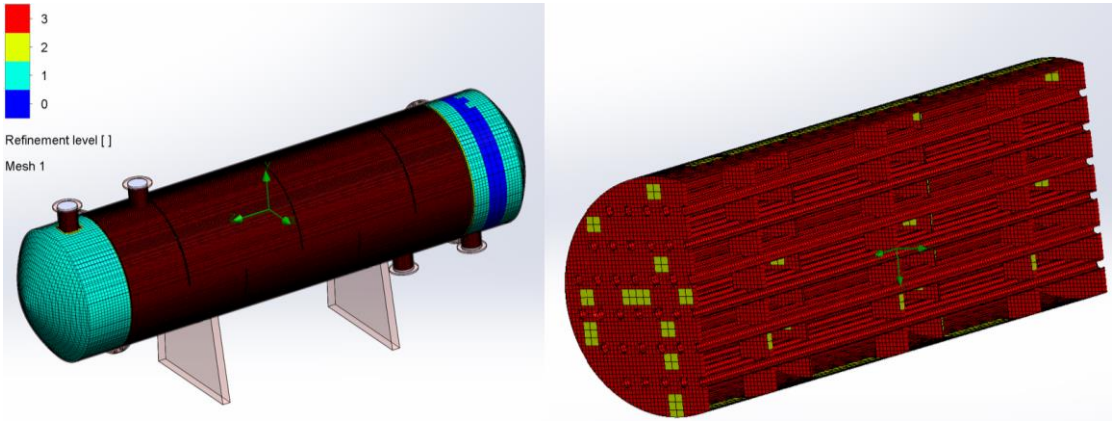

(a) (b)

Fig. 8. (a) Mesh results on 3D-level refinement (b) Mesh results on heat exchanger tubes

ii. Fluid selections

Regarding the choice of fluids, in the first case study, only water will be used (see Table 3), whereas hot water will be utilized to heat cold water. In the second case, the TiO_2 nanofluid will be used (see Table 4) within the water at a concentration of 0.5%.

Table 3
Water thermal properties [23]

Material	ρ k g/m3	Cp J/kg K	K W/m K	μ Pa.s
Water-liquid	997	4180	0.63	0.000404

Table 4
Thermal properties of (TiO_2) nanoparticles [24]

Specification	Value
Clarity	99.50%
Molecular weight	79. 7 $Gr\ mol^{-1}$
Diameter	21 Nm
Density	4250 kg/m^{-3}
Thermal conductivity	8.9 $Wm^{-1}K^{-1}$
Specific Heat	686.2 $J/kg^{-1}K^{-1}$

The concentration of TiO_2, which is the nanofluid used in this research, is 0.5%, with water serving as the base fluid. Utilizing Eq. (12) to Eq. (15), the thermophysical properties of the nanofluid were calculated and are illustrated in the Table 5. This methodical approach ensures a precise understanding of the nanofluid's characteristics, which is important for the study's accuracy and relevance.

Table 5
Thermal properties TiO_2 nanofluid with a concentration of 0.5%

Material	ρ kg/m3	Cp J/kg K	k W/m.K	μ Pa.s
TiO_2 with ϕ 0.5%	1013.256	4164.521	0.65	0.0010125

iii. Boundary conditions

The Figure 9 below shows the boundary conditions for the cold and hot fluid inlet. Table 6 illustrate fluids in both case studies and their boundary conditions

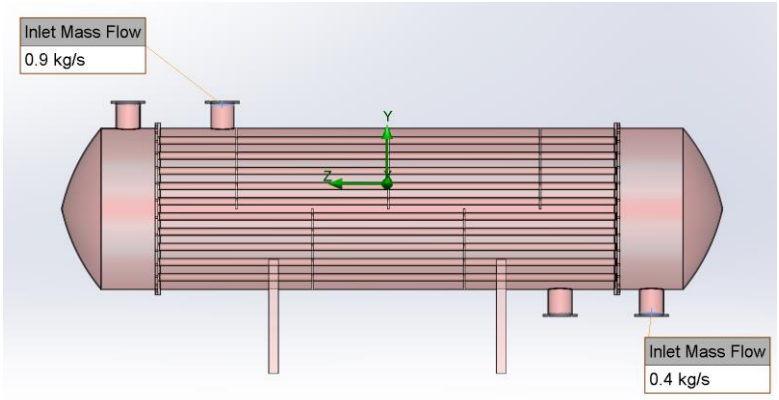

Fig. 9. Shows the inlet mass flow rate for the cold and hot fluids

Table 6
Fluids in both case studies and their boundary conditions

Fluid	Fluid	Temperature	Mass flow rate
Case Study 1	Hot fluid: water	65 C	0.9 kg/s
	Cold fluid: water	15 C	0.4 kg/s
Case study 2	Hot fluid: TiO_2 with ϕ 0.5%	65 C	0.9 kg/s
	Cold fluid: water	15 C	0.4 kg/s

3. Results

In this section, the key findings of the study will be presented and discussed. First, the case of utilizing hot water to heat cold water will be examined in detail. Subsequently, the alternative case will be analysed and compared with the initial case to highlight the differences and similarities between the two approaches. By presenting the results in a systematic and comparative manner, this section aims to provide a comprehensive understanding of the investigated heating methods and their respective performance characteristics.

3.1 First Case Study Results

3.1.1 Grid test results

The results of the grid test, which compares the number of cells listed in Table 2 with the outlet temperature of the cold fluid after heating, will be presented. The outlet temperature is considered the most important parameter in this study.

Table 7, located below Figure 10, show the outlet temperatures of the cold fluid after heating for different numbers of cells, which correspond to the mesh refinement levels. Both the figure and the table show that the curve becomes stable between approximately 4,112,679 and 9,419,425 cells. As a result, **9,419,425** was chosen as the optimal number of cells, representing the best mesh to use for the rest of the analysis. This choice shows the careful method used to make sure the thermal analysis is accurate and efficient.

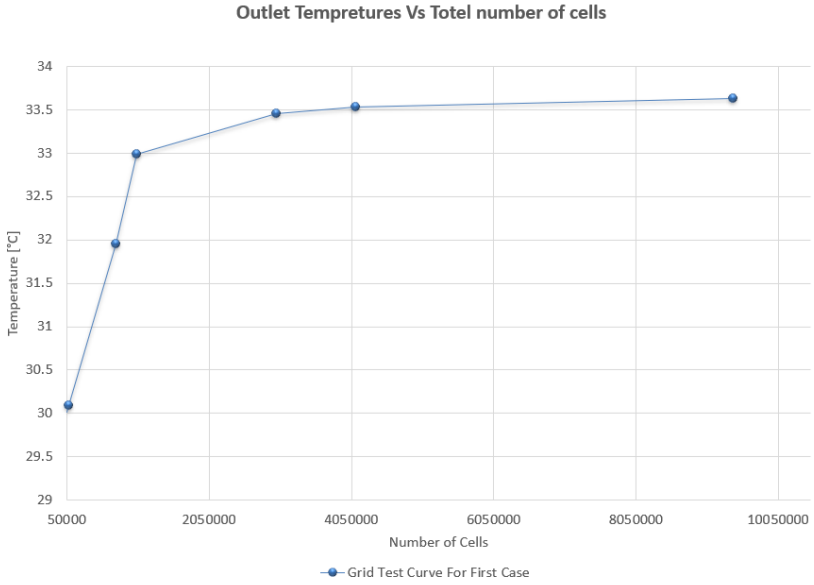

Fig. 10. Outlet temperatures for cold fluid at different numbers of cells in the first case

Table 7
Outlet temperature values for different numbers of cells for the first case

Refinement level	Number of cells	Temperature
1	45816	30.0148 C
2	71428	30.0929 C
3	734358	31.9548 C
4	1029859	32.9914 C
5	2989859	33.4184 C
6	4112679	33.5632 C
7	9419425	33.6301 C

3.1.2 Temperatures results and distribution

The Figure 11 below shows the temperature changes of hot water after it loses energy to cold water.

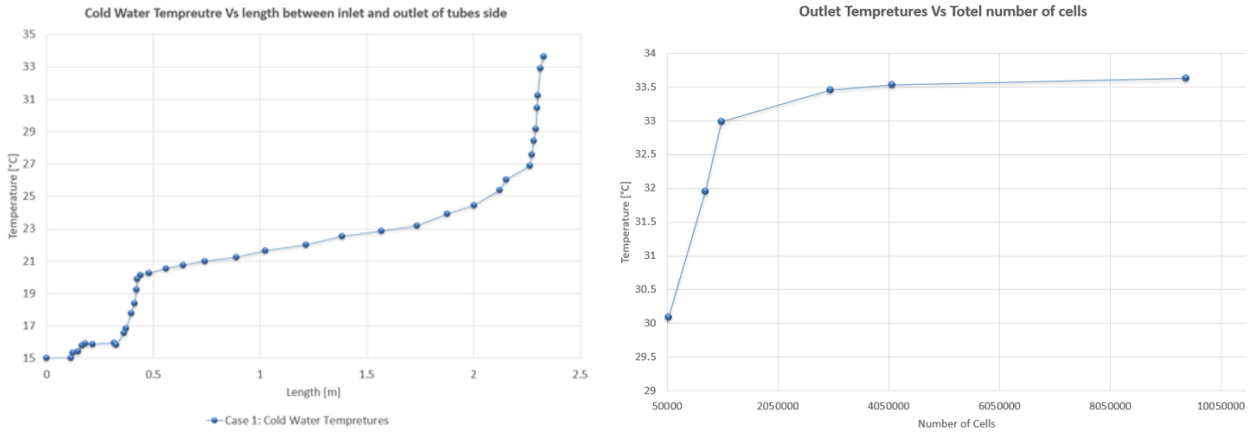

(a) (b)

Fig. 11. Temperature results for the first case study (a) Temperatures decrease for hot fluid on the shell side between the inlet and outlet (b) Temperatures rise for cold fluid in the tube between the inlet and outlet

The Figure 12 and Figure 13 below show the temperature contours for the first case study. The first figure illustrates the temperatures at the inlet, which were also set as boundary conditions. The figure below shows the resultant temperatures in both the cold and hot fluids.

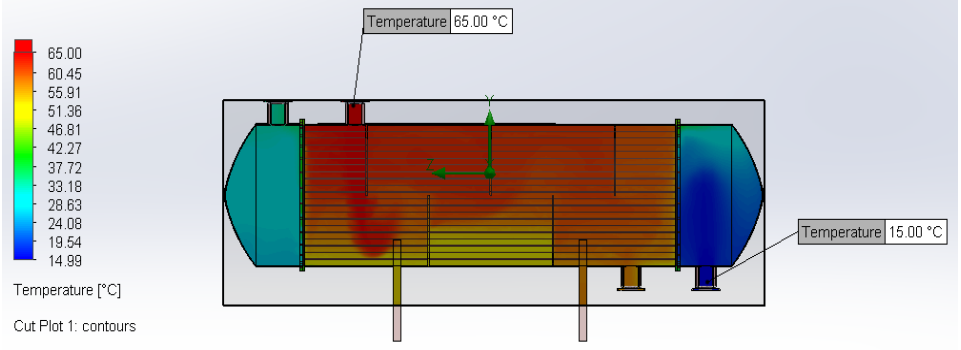

Fig. 12. Temperature contours results and inlet temperatures for both fluids

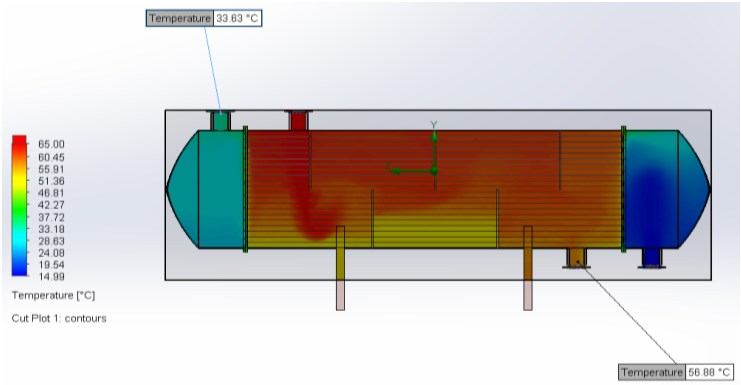

Fig. 13. Temperature contour results and outlet temperatures for both fluids in the first case

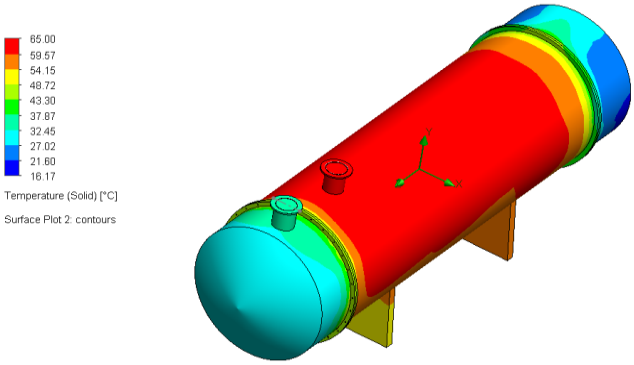

Fig. 14. Surface temperature distribution on the shell and tube heat exchanger in the first case

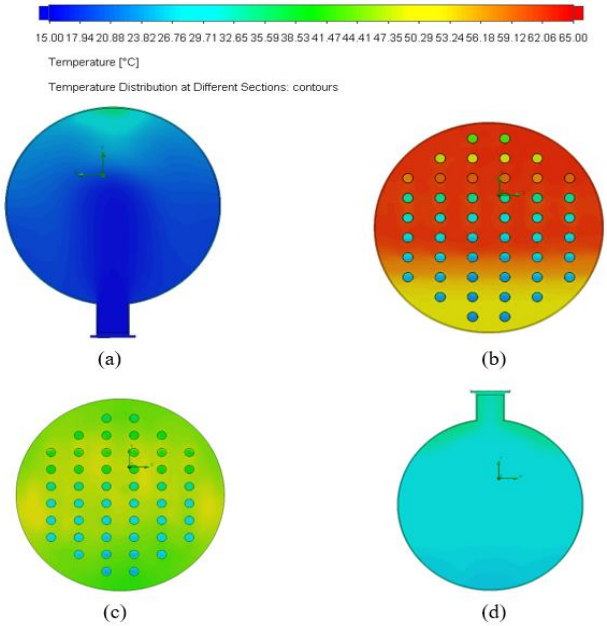

Fig. 15. (a) Temperature distributions at the tube side inlet (b) temperature distribution at the midpoint of the heat exchanger (c) temperature distribution at the end of the shell side (d) temperature distribution at the tube side outlet

The Figure 14 shows the heat distribution on the outer surface of the shell and tube-type heat exchanger. This distribution depends on the metal the exchanger is made of, which in this case is copper. As noted, the highest temperatures are in the central region, and the reason is that it is the entrance to the hot fluid.

Figure 15 illustrates the temperature distribution from the cold-water inlet to the outlet along the shell-and-tube heat exchanger after several sections have been taken.

3.2 Second Case Study Results

3.2.1 Grid test results

A grid test will also be conducted for the second case study, due to the difference in fluid used here. In this scenario, the hot water will be replaced with hot water mixed with nanomaterials, making the fluid in this case a 0.5% concentration of TiO_2. Its properties have been calculated and are presented in Table 3 above. The results are shown in the Figure 16 and Table 8 below.

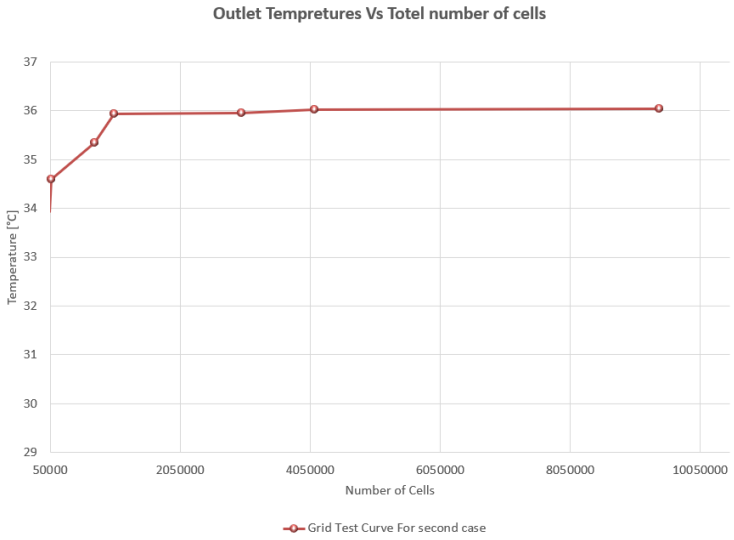

Fig. 16. Outlet temperature for cold fluid at different numbers of cells

Table 8
Outlet temperature values for different numbers of cells in the second case

Refinement level	Number of cells	Temperature
1	45816	33.92498
2	71428	34.5929
3	734358	35.3448
4	1029859	35.9414
5	2989859	35.9602
6	4112679	36.04332
7	9419425	36.0509

It is observed from Figure 16 above that the curve stabilized when the number of cells equaled **4,112,679,** with a temperature at that point being **36.04°C**, which is also detailed in Table 8 above. This indicates that this is the optimum mesh for the second case study, upon which the simulation will proceed.

3.2.2 Temperatures results and distribution

Figure 17 below shows the change in temperature of the hot fluid, which is water containing 0.5% titanium dioxide (TiO_2) nanoparticles, as it heats the cold water.

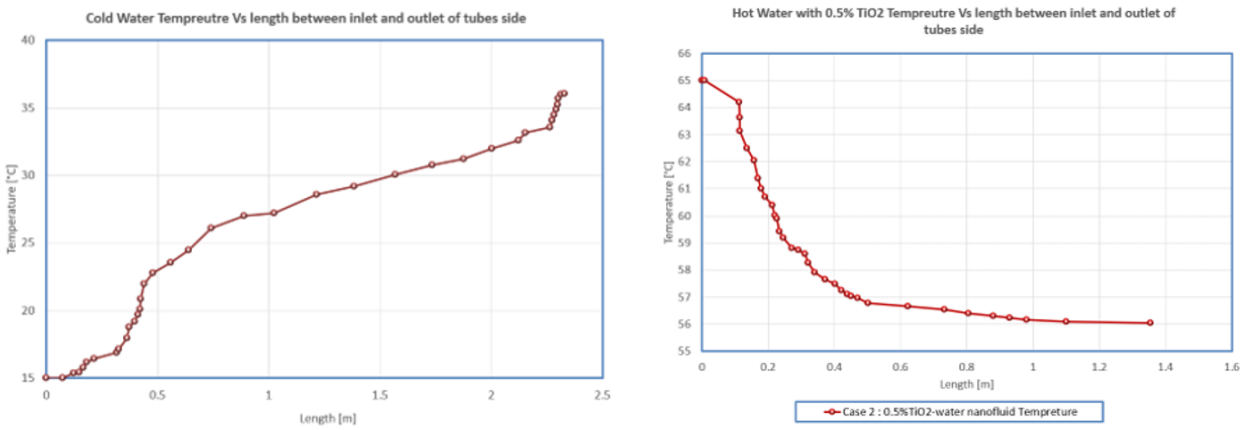

(a) (b)

Fig. 17. Temperature results for the second case study (a) Rise in cold fluid temperatures from inlet to outlet in the tube (b) Decrease in hot fluid temperatures from inlet to outlet on the shell side

Figure 18 below illustrates the final temperatures of the cold and hot water in the second case study.

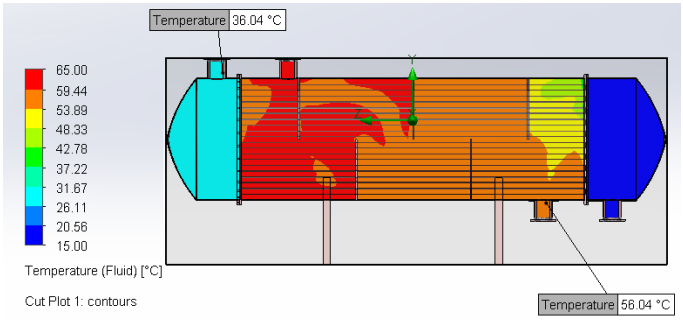

Fig. 18. Temperature contour results and outlet temperatures for both fluids in the second case

Figure 19 below illustrates the temperature distribution across the surface of the heat exchanger in the second case study.

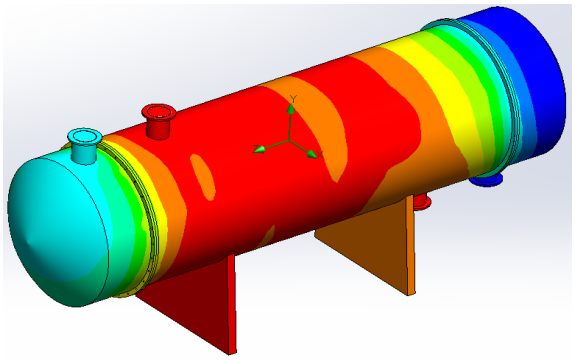

Fig. 19. Surface temperature distribution on the shell and tube heat exchanger for the second case

The Figure 20 below shows the temperature distribution along different sections at several locations along the z direction for the second case study. Table 9 illustrates results for both case studies.

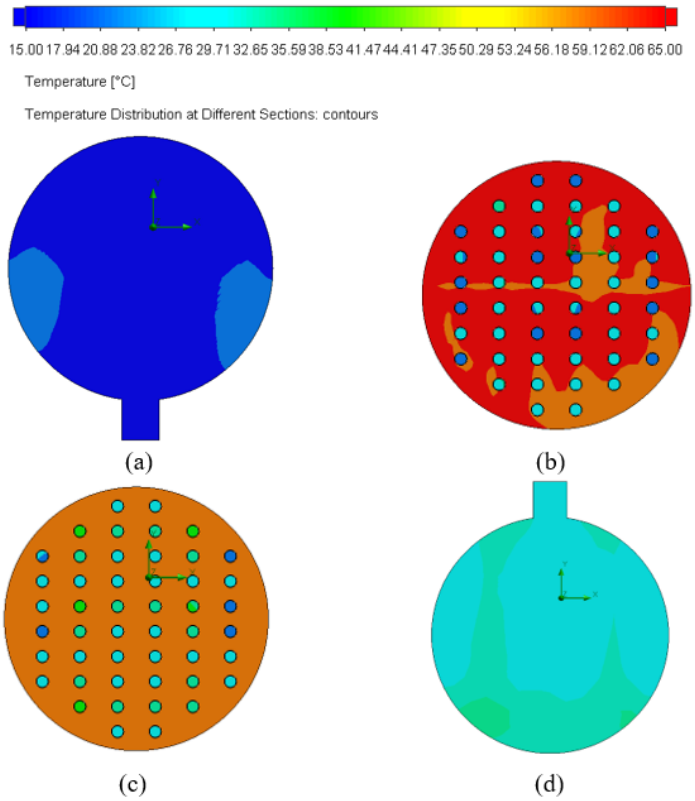

Fig. 20. (a) Temperature distribution at the tube side inlet (b) Temperature distribution at the midpoint of the heat exchanger (c) Temperature distribution at the end of the shell side (d) Temperature distribution at the tube side outlet

Table 9
Results for both case studies

Case	Fluid	Outlet temperature
Case Study 1	Hot fluid: water	56.88 C
	Cold fluid: Water	33.63 C
Case study 2	Hot fluid: TiO_2 with ϕ 0.5%	56.04 C
	Cold fluid: Water	36.04 C

To calculate the percentage improvement in heat transfer, the formula used is:

$$\text{Improvement Percentage} = \frac{(\Delta T_{second\ case} - \Delta T_{first\ case})}{\Delta T_{first\ case}} \times 100\% \quad (21)$$

$$\text{Improvement Percentage} = \frac{((36.04 - 15) - (33.63 - 15))}{(33.63 - 15)} \times 100\% = \mathbf{11.44\%}$$

Here is the revised interpretation of the results, addressing the reviewer's comment and maintaining a logical flow without mentioning experimental data: The CFD simulations demonstrate the enhanced heat transfer performance of the shell and tube heat exchanger when using a 0.5% TiO_2 nanofluid compared to pure water. The results show that the nanofluid increases the outlet temperature of the cold fluid by 11.44% (36.04°C) compared to water (33.63°C). This significant improvement can be attributed to the unique thermophysical properties of the nanofluid, such as increased thermal conductivity and convective heat transfer coefficient. The accuracy of the CFD model is validated by its ability to predict key heat transfer parameters, including local heat transfer coefficients, fluid bulk temperatures, and surface heat fluxes. The grid independence study, which compares multiple mesh resolutions, ensures that the solution is not influenced by the mesh size and that the results are physically meaningful. The detailed temperature contours and profiles obtained from the CFD simulations provide valuable insights into the spatial variations of heat transfer along the length of the heat exchanger and within the nested fluid passages. These results help to identify regions of high and low heat transfer, which can be used to optimize the design of the heat exchanger. The contours also reveal the complex interplay between the thermal and hydraulic phenomena occurring within the system. The enhanced heat transfer performance of the nanofluid comes at the cost of increased viscosity, which can lead to higher pumping power requirements. However, the results suggest that the benefits of the nanofluid, such as improved heat transfer and potentially smaller heat exchanger sizes, may outweigh the drawbacks in certain applications. Further parametric analyses can help to optimize the system by finding the ideal balance between heat transfer enhancement and pressure drop. The CFD simulations provide a powerful tool for analysing and developing nanofluid-based heat exchangers. The accurate capture of the underlying physics enables researchers and engineers to make informed decisions about the use of nanofluids in specific heat transfer applications. Further studies, including experimental validation, are necessary to assess the practical feasibility of nanofluid-enhanced heat exchangers in real-world conditions and to confirm the simulation results.

4. Conclusions

In conclusion, this computational study demonstrates the potential of TiO_2 nanofluids to enhance the thermal performance of shell-and-tube heat exchangers. The CFD analysis revealed that adding TiO_2 nanoparticles at a concentration of 0.5% led to an 11.44% improvement in heat transfer efficiency compared to the base fluid. The numerical results were validated through grid independence testing and closely agreed with experimental correlations, confirming the accuracy of the CFD approach. The key innovation lies in the successful integration of TiO_2 nanofluids with an optimized heat exchanger design, identifying the optimal nanoparticle concentration (0.5%) that maximizes heat transfer enhancement. Future research should explore varying nanoparticle concentrations, investigate other nanoparticle materials, and validate the findings experimentally. This study lays the foundation for developing high-performance, nanofluid-enhanced heat exchangers that can significantly improve energy efficiency in various industrial sectors. By harnessing the unique properties of nanofluids, this innovative approach has the potential to revolutionize heat transfer technologies and contribute to more sustainable and cost-effective industrial processes.

Acknowledgement
This research was fully funded by Altinbas University.

References

[1] T. Alaquainc, "Top 10 Benefits of Using Heat Exchanger in Industrial Processes," Alaquainc.
[2] Heydari, Ali, Mostafa Shateri, and Sina Sanjari. "Numerical analysis of a small size baffled shell-and-tube heat exchanger using different nano-fluids." *Heat transfer engineering* 39, no. 2 (2018): 141-153. https://doi.org/10.1080/01457632.2017.1288052
[3] Rani, G. Jamuna, G. Sai Rani, and Anchupogu Praveen. "Nano fluids effect on crossflow heat exchanger characteristics–Review." *Materials Today: Proceedings* 44 (2021): 527-531. https://doi.org/10.1016/j.matpr.2020.10.210
[4] Kareemullah, Mohammed, K. M. Chethan, Mohammed K. Fouzan, B. V. Darshan, Abdul R. Kaladgi, Maruthi BH Prashanth, Rayid Muneer, and K. M. Yashawantha. "Heat transfer analysis of shell and tube heat exchanger cooled using nanofluids." *Recent Patents on Mechanical Engineering* 12, no. 4 (2019): 350-356. https://doi.org/10.2174/2212797612666190924183251
[5] Lahari, MLR Chaitanya, PHV Sesha Talpa Sai, and Harish Makena. "Design and Analysis of Hair Pin Heat Exchanger using TiC, MgO, Ag/Water-Glycerin Nano Fluids." https://doi.org/10.17577/ijertv7is010089
[6] Ghazanfari, Valiyollah, Armin Taheri, Younes Amini, and Fatemeh Mansourzade. "Enhancing heat transfer in a heat exchanger: CFD study of twisted tube and nanofluid (Al2O3, Cu, CuO, and TiO2) effects." *Case Studies in Thermal Engineering* 53 (2024): 103864. https://doi.org/10.1016/j.csite.2023.103864
[7] Hussein, Diyar F., and Yaser Alaiwi. "Efficiency Improvement of Double Pipe Heat Exchanger by using TiO2/water Nanofluid." *CFD Letters* 16, no. 1 (2024): 43-54. https://doi.org/10.37934/cfdl.16.1.4354
[8] Ghazanfari, V., M. Talebi, J. Khorsandi, and R. Abdolahi. "Thermal–hydraulic modeling of water/Al2O3 nanofluid as the coolant in annular fuels for a typical VVER-1000 core." *Progress in Nuclear Energy* 87 (2016): 67-73. https://doi.org/10.1016/j.pnucene.2015.11.008
[9] Çengel, Y. A., and A. J. Ghajar. "Heat and Mass Transfer: Fundamentals [and] Applications. New York City." (2020).
[10] Bergman, Theodore L. *Fundamentals of heat and mass transfer*. John Wiley & Sons, 2011.
[11] Kakaç, S., Liu, H., & Pramuanjaroenkij, A. (2020). Heat Exchangers: Selection, Rating, and Thermal Design, Fourth Edition (4th ed.). CRC Press. https://doi.org/10.1201/9780429469862
[12] Nitsche, Manfred, and Raji Olayiwola Gbadamosi. *Heat exchanger design guide: a practical guide for planning, selecting and designing of shell and tube exchangers*. Butterworth-Heinemann, 2015.
[13] Ali, Abu Raihan Ibna, and Bodius Salam. "A review on nanofluid: preparation, stability, thermophysical properties, heat transfer characteristics and application." *SN Applied Sciences* 2, no. 10 (2020): 1636. https://doi.org/10.1007/s42452-020-03427-1
[14] Pordanjani, Ahmad Hajatzadeh, Saeed Aghakhani, Masoud Afrand, Boshra Mahmoudi, Omid Mahian, and Somchai Wongwises. "An updated review on application of nanofluids in heat exchangers for saving energy." *Energy Conversion and Management* 198 (2019): 111886. https://doi.org/10.1016/j.enconman.2019.111886
[15] Saidur, Rahman, K. Y. Leong, and Hussein A. Mohammed. "A review on applications and challenges of nanofluids." *Renewable and sustainable energy reviews* 15, no. 3 (2011): 1646-1668. https://doi.org/10.1016/j.rser.2010.11.035
[16] Raja, RA Arul, J. Sunil, M. Hamilton, and J. Davis. "Estimation of thermal conductivity of nanofluids using theoretical correlations." *Int. J. Appl. Eng. Res* 13, no. 10 (2018): 7932-7936.
[17] Breki, Alexander, and Michael Nosonovsky. "Einstein's viscosity equation for nanolubricated friction." *Langmuir* 34, no. 43 (2018): 12968-12973. https://doi.org/10.1021/acs.langmuir.8b02861
[18] Akilu, S., A. T. Baheta, K. V. Sharma, and M. A. Said. "Experimental determination of nanofluid specific heat with SiO2 nanoparticles in different base fluids." In *AIP conference proceedings*, vol. 1877, no. 1. AIP Publishing, 2017. https://doi.org/10.1063/1.4999896
[19] Hamid, K. Abdul, W. H. Azmi, Rizalman Mamat, N. A. Usri, and G. Najafi. "Effect of temperature on heat transfer coefficient of titanium dioxide in ethylene glycol-based nanofluid." *Journal of Mechanical Engineering and Sciences* 8 (2015): 1367-1375. https://doi.org/10.15282/jmes.8.2015.11.0133
[20] Blazek, Jiri. *Computational fluid dynamics: principles and applications*. Butterworth-Heinemann, 2015.
[21] W. Versteeg, H. K., & Malalasekera, *An Introduction to Computational Fluid Dynamics*, 2nd ed. London: Pearson Education Limited, 2007.
[22] Lee, Minhyung, Gwanyong Park, Changyoung Park, and Changmin Kim. "Improvement of grid independence test for computational fluid dynamics model of building based on grid resolution." *Advances in Civil Engineering* 2020, no. 1 (2020): 8827936. https://doi.org/10.1155/2020/8827936
[23] Borgnakke, Claus, and Richard E. Sonntag. *Fundamentals of thermodynamics*. John Wiley & Sons, 2020.

[24] Permanasari, Avita Ayu, Brilian Shakti Kuncara, Poppy Puspitasari, Sukarni Sukarni, Turnad Lenggo Ginta, and Windra Irdianto. "Convective heat transfer characteristics of TiO2-EG nanofluid as coolant fluid in heat exchanger." In *AIP conference proceedings*, vol. 2120, no. 1. AIP Publishing, 2019. https://doi.org/10.1063/1.5115691